SZENT ISTVÁN UNIVERSITY

Modelling the Static and Dynamic Operation of Pneumatic Artificial Muscles and Their Accurate Positioning

Thesis of PhD Dissertation

József Sárosi

Gödöllő
2013

Doctoral School

denomination: Mechanical Engineering PhD School

science: Agricultural Technical Science

leader: Dr. István Farkas
professor, DSc
Faculty of Mechanical Engineering
Szent István University, Gödöllő, Hungary

supervisor: Dr. Péter Szendrő
professor, DSc
Faculty of Mechanical Engineering
Szent István University, Gödöllő, Hungary

co-supervisor: Dr. Gábor Keszthelyi-Szabó
professor, DSc
Faculty of Engineering
University of Szeged, Szeged, Hungary

………………………………..   …………………………………

Affirmation of the Doctoral School
leader   Affirmation of supervisor

CONTENT

NOMENCLATURE AND ABBREVATIONS

Nomenclature:

$a_1, a_2, a_3, a_4, a_5, a_6$	constants
c [N·s·m^{-1}]	damping coefficient
c_{cr} [N·s·m^{-1}]	critical damping coefficient
F [N]	force
F_a [N]	force determined by hysteresis loop lower curve
F_f [N]	force determined by hysteresis loop upper curve
F_{spring} [N]	the force exerted by the PAM as spring
g [m·s^{-2}]	acceleration of gravity
k [N·m^{-1}]	stiffness
l [m]	length when the PAM is contracted
l_0 [m]	nominal length
m [kg]	mass
p [Pa]	applied pressure
R [-]	correlation coefficient
U [-]	surface
x [m]	displacement

Greek symbols:

ζ [-]	damping ratio
κ [%]	contraction

Abbreviations:

LabVIEW	Laboratory Virtual Instrumentation Engineering Workbench
PAM	Pneumatic Artificial Muscle

1. INTRODUCTION AND OBJECTIVES

Lately interest has increased in the so called contracting - pistonless - pneumatic cylinders also known as pneumatic artificial muscles (PAMs). These pneumatic actuators play an important role in industry applications (e.g. hole punchers, winders, lifting mechanisms, vibrating funnels) but also in the fields of medicine (e.g. moving artificial limbs) and robotics (e.g. jumping and bipedal robots).

When I decided on the topic for my Dissertation I set out to gather deeper knowledge of pneumatic artificial muscles from the great number of literature from these formulate the possible directions in which I can find new results which can be used in industrial applications. Thus the goals can be summed up as:

1. Design and implement a multifunctional universal measurement systems hardware and software which can singularly gather those characteristics of the PAMs which describe it (e.g. pressure, position (linear and angular), force, surface temperature, internal temperature) and can be used for high accuracy positioning. The system has to be able to measure PAMs most descriptive feature the force-contraction diagram at constant pressure which is important for goal number 2. The general purpose hardware and software system should be applicable in new research fields and education.
2. Implement an algorithm to approximate the static force exerted by the PAM for all diameters, lengths and pressures.
3. Develop a dynamic model which describes the behaviour of PAMs. The purpose of which is to study the stiffness and damping coefficient of PAMs, also it should also describe the whole system containing PAM.
4. Achieve positioning precision greater than that found in literature (0,01 mm linear and 0,036° angular).
5. Examine those phenomena that may influence the positioning precision (e.g. changing temperature, hysteresis).

2. MATERIAL AND METHOD

In the chapter *Material and Method* the hardware and software systems of the device for measuring PAMs will be introduced along with the experiments and their configuration, the new model for the approximation of the static force, the possibilities of examining dynamic behaviour and the applied methods.

2.1. Experimental Setup

To understand and examine the attributes, behaviour, parameters and their function like connection I developed a measurement system. Its hardware and software systems can be seen on Figures 2-1, 2-2, 2-4, 2-5 and 2-6. For my research I used several of Festo brand patented Fluidic Muscles: DMSP-10-250N-RM-RM (10 mm diameter, 250 mm length), DMSP-20-200N-RM-RM (20 mm diameter, 200 mm length) and DMSP-20-400N-RM-RM (20 mm diameter, 400 mm length).
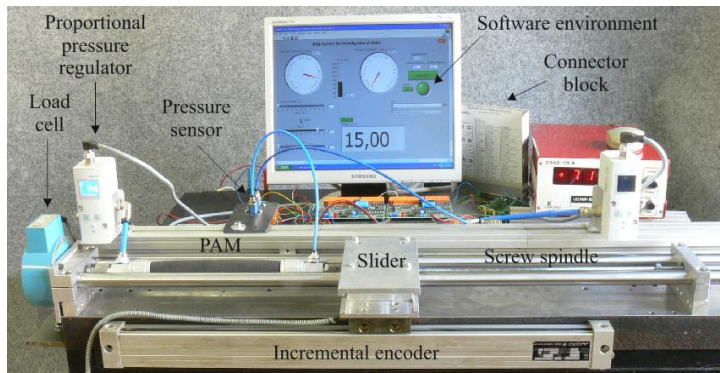

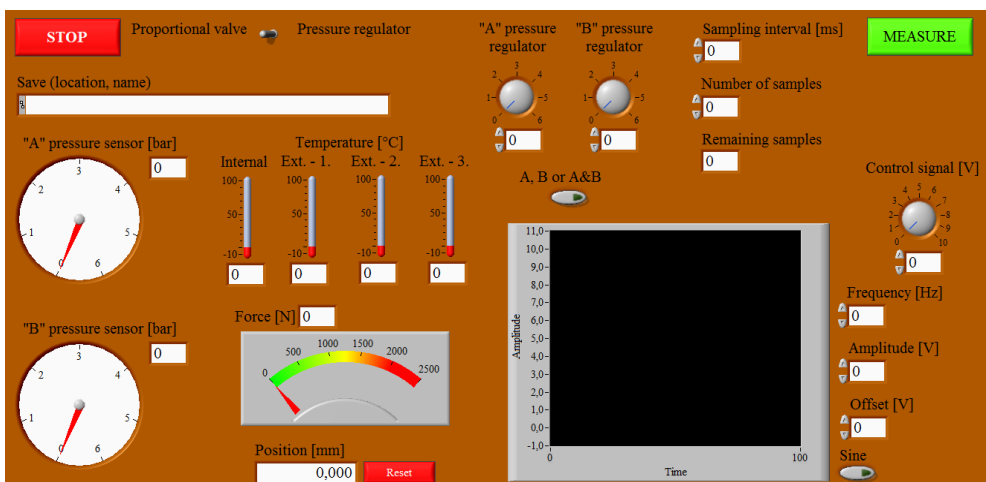Figure 2-1: Experimental setup for investigation of PAMs

Figure 2-2: Front panel of LabVIEW program for measuring pressure, force, position and temperature's effect on positioning

To acquire the force-contraction characteristic of the PAMs they were placed horizontally, one end was attached to the load cell the other end could move freely. The free end was attached to a threaded rod so that I could adjust the position freely which was detected with a LINIMIK MSA 320 type incremental encoder at a precision of 0,01 mm. The output signal (force) varied with the direction of the input signal (position), in other words I detected hysteresis. The force-contraction curve was sampled in 30 points. The measurements were done at room temperature as well as repeated five times and taken the average according to accepted research methodology.

2.2. Static Force Model of Pneumatic Artificial Muscles

The function to compute the force exerted by the PAM can yield valuable information during the dimensioning of components since without measurements we can calculate at given contraction and pressure the exerted force of the PAM.

I developed a new function for the force:

$$F(p,\kappa) = (a_1 \cdot p + a_2) \cdot \exp^{a_3 \cdot \kappa} + a_4 \cdot \kappa \cdot p + a_5 \cdot p + a_6, \qquad (2.1)$$

where: p applied pressure, κ contraction (relative displacement), a_1, a_2, a_3, a_4, a_5 and a_6 unknown parameters.

The unknown constants of the described function have been calculated with MS Excel 2010 (Solver) which does not require programming knowledge. The pressure is substituted in bar while the contraction in %. The unknown constants a_1, a_2, a_3, a_4, a_5 and a_6 confidence interval, meaning their upper and lower limits have been calculated with MS Excel 2010 Data Analysis add-in with 95 % accuracy. I also examined the closeness of the fit of the calculated and measured data as well as the errors function like nature.

2.3. Dynamic Investigation of Pneumatic Artificial Muscles

For the dynamic analysis of PAMs let us look at the system depicted on Figure 2-3.
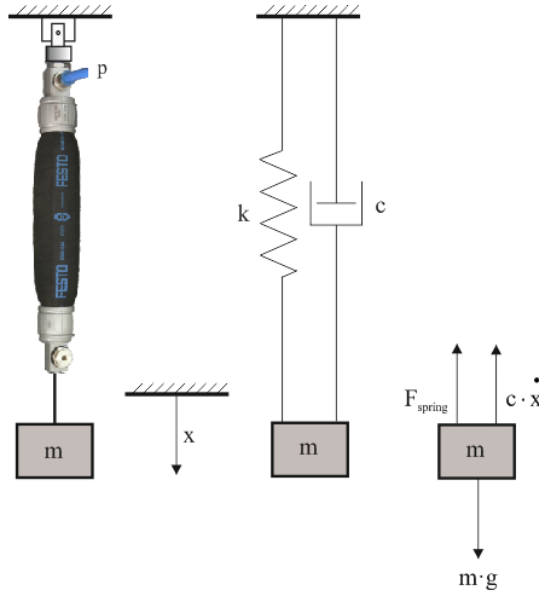
Figure 2-3: PAM as a lifting device and its model

The pendulous system which is vertical and has one degree of freedom can be described with the following differential equation:

$$m \cdot \ddot{x} = -F_{spring}[\kappa(x)] - c[\kappa(x)] \cdot \dot{x} + m \cdot g ,$$ (2.2)

where: F_{spring} the force exerted by the PAM as spring which can be calculated by equation (2.1), x displacement, m mass, c damping coefficient, g acceleration of gravity.

To analyse the nonlinear model first we must determine the c damping coefficient function from equation (2.2). For this I use the force-contraction functions hysteresis loop. Let F_f be the loops upper curve and F_a the loops lower curve, then the U_0 surface which is under F_f can be calculated with equation (2.1) (p = const.):

$$U_0 = l_0 \cdot \int_{\kappa_{min}}^{\kappa_{max}} F_f(\kappa)d\kappa = l_0 \cdot \int_{\kappa_{min}}^{\kappa_{max}} F_f(p,\kappa)d\kappa =$$

$$= l_0 \cdot \int_{\kappa_{min}}^{\kappa_{max}} [(a_1 \cdot p + a_2) \cdot exp^{a_3 \cdot \kappa} + a_4 \cdot \kappa \cdot p + a_5 \cdot p + a_6]d\kappa =$$

$$= l_0 \cdot \left[\frac{2 \cdot a_1 \cdot p \cdot exp^{a_3 \cdot \kappa_{max}} + 2 \cdot a_3 \cdot a_6 \cdot \kappa_{max} + 2 \cdot a_2 \cdot exp^{a_3 \cdot \kappa_{max}} + 2 \cdot a_3 \cdot a_5 \cdot p \cdot \kappa_{max} + a_3 \cdot a_4 \cdot p \cdot \kappa_{max}^2}{2 \cdot a_3} \right] -$$

$$l_0 \cdot \left[\frac{2 \cdot a_1 \cdot p \cdot exp^{a_3 \cdot \kappa_{min}} + 2 \cdot a_3 \cdot a_6 \cdot \kappa_{min} + 2 \cdot a_2 \cdot exp^{a_3 \cdot \kappa_{min}} + 2 \cdot a_3 \cdot a_5 \cdot p \cdot \kappa_{min} + a_3 \cdot a_4 \cdot p \cdot \kappa_{min}^2}{2 \cdot a_3} \right].$$ (2.3)

8

The area of curve can be calculated:

$$\Delta U = U_0 - l_0 \cdot \int_{\kappa_{min}}^{\kappa_{max}} F_a(\kappa) d\kappa. \tag{2.4}$$

The ζ damping ratio:

$$\zeta = \frac{\Delta U}{U_0}. \tag{2.5}$$

The critical damping coefficient (c_{cr}):

$$c_{cr} = 2 \cdot \sqrt{k \cdot m}, \tag{2.6}$$

where k stiffness which can be calculated by equation (2.1):

$$k = k(\kappa) = \frac{dF(l)}{dl} = \frac{dF(\kappa)}{l_0 \cdot d\kappa} = \frac{1}{l_0} \cdot \frac{dF(\kappa)}{d\kappa}, \tag{2.7}$$

$$\frac{dF(\kappa)}{d\kappa} = \frac{dF(p,\kappa)}{d\kappa} = \frac{d[(a_1 \cdot p + a_2) \cdot \exp^{a_3 \cdot \kappa} + a_4 \cdot \kappa \cdot p + a_5 \cdot p + a_6]}{d\kappa} = $$
$$= (a_1 \cdot p + a_2) \cdot a_3 \cdot \exp^{a_3 \cdot \kappa} + a_4 \cdot p \, (p = \text{const.}) \tag{2.8}$$

$$k(\kappa) = \frac{(a_1 \cdot p + a_2) \cdot a_3 \cdot \exp^{a_3 \cdot \kappa} + a_4 \cdot p}{l_0}. \tag{2.9}$$

The c damping coefficient:

$$\zeta = \frac{c}{c_{cr}} \rightarrow c = \zeta \cdot c_{cr}. \tag{2.10}$$

Since at a given pressure the F_{spring} force, the stiffness and damping coefficient change as a function of contraction - which is a function of displacement x - I developed a model that takes these into consideration.

2.4. Accurate Positioning of Pneumatic Artificial Muscles

PAMs can be used in applications where high accuracy positioning is necessary. Due to the nonlinearity a robust control is needed. In this chapter I present the experiments associated with the positioning of PAMs, their measurement configuration as well as their LabVIEW based sliding-mode control.

2.4.1. Linear Positioning of Pneumatic Artificial Muscles

For the linear positioning of the PAMs I used two DMSP-20-200N-RM-RM type muscles which were controlled by a Festo brand MPYE-5-1/8 HF-010B type 5/3 proportional valve. Linear positioning done with the PAMs in an antagonistic configuration is depicted in Figure 2-4.
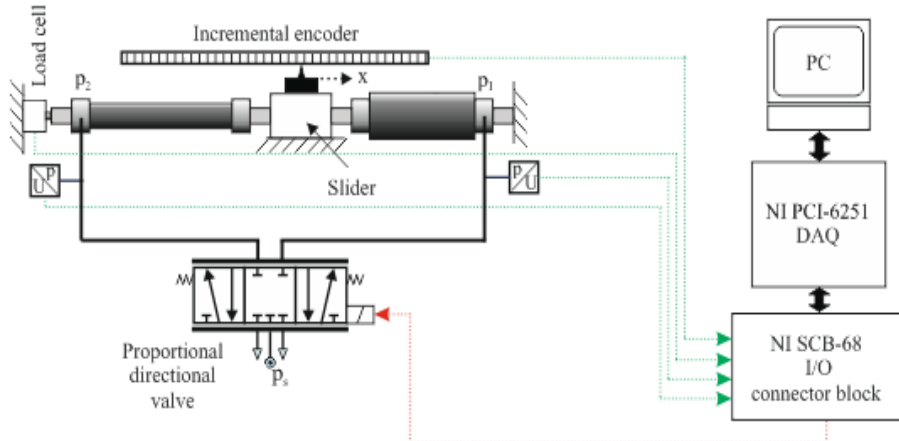

Figure 2-4: Linear positioning with proportional control valve

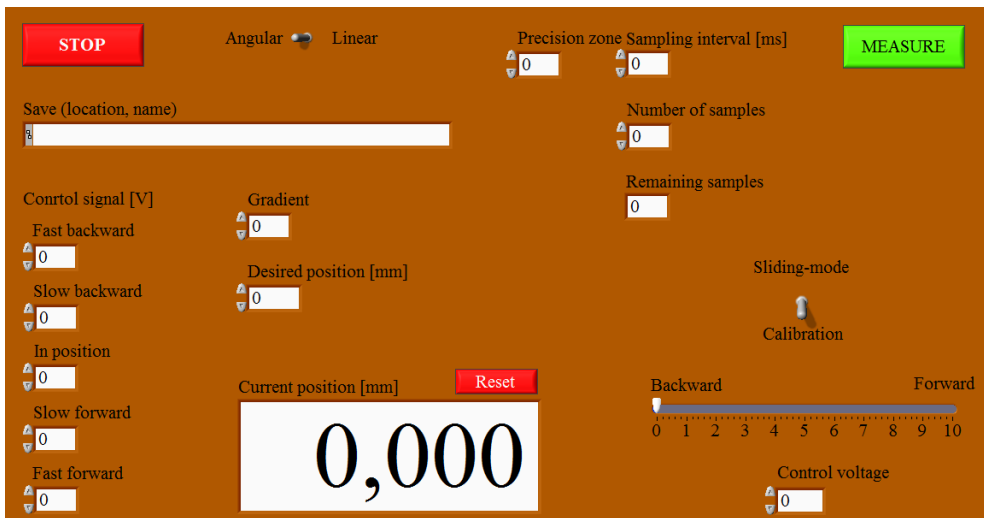Figure 2-5 shows the front panel of the LabVIEW program containing the sliding-mode control.

Figure 2-5: Front panel of the LabVIEW program for investigation of positioning

The values of the input signal used to control the proportional valve are as follows: fast backward (4 V), slow backward (4,65 V), in position (5 V), slow forward (5,35 V) and fast forward (6 V).

10

2.4.2. Investigation of Temperature Change and Hysteresis

I also examined such phenomena which are believed to influence the accuracy of the positioning, such as changing temperature as well as hysteresis.

As depicted in Figure 2-6 I built in a single DMSP-20-400N-RM-RM type PAM into the experimental rig. For the periodic movement as well as the monitoring of internal and external temperatures I used the LabVIEW program depicted in Figure 2-2.
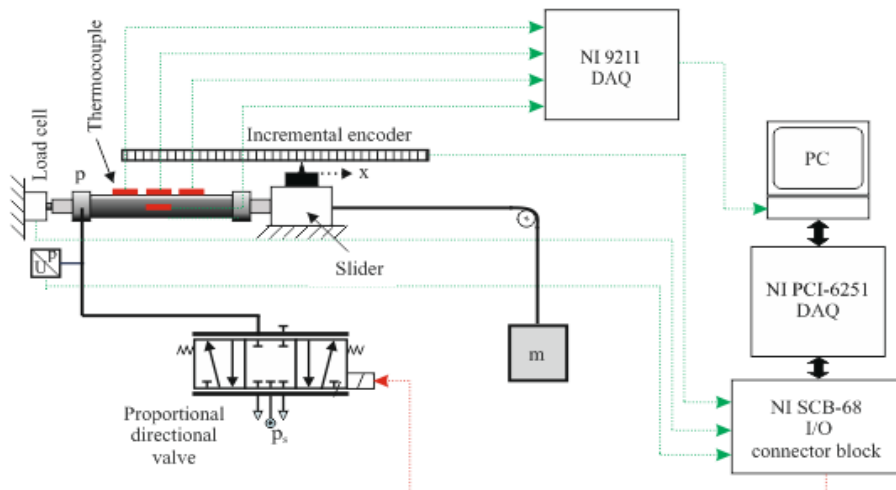

Figure 2-6: Investigation of temperature change

I compared the internal and external temperatures of the PAMs at different frequencies (0,1 Hz, 0,25 Hz, 0,5 Hz, 0,75 Hz and 1 Hz). In all cases I cooled the temperature of the PAM to -10 °C with a Novasol M5 type compressed air spray while the moved load was 20 kg.

I also used this experimental setup to measure the effect of hysteresis on the accuracy of the positioning. My measurements were done at room temperature and with a load of m = 20 kg.

2.4.3. Positioning of Pneumatic Artificial Muscles with Rotary Encoder

Often as a result of the air fed inside the PAMs the movement is not linear but angular. To measure this I built a different antagonistic configuration with DMSP-10-250N-RM-RM type PAMs. The angular displacement was measured with an incremental encoder which can achieve a precision of 0,036°. For this measurement the LabVIEW program illustrated in Figure 2-5 is required. The measurements were also made at room temperature.

3. RESULTS

In this section I sum up the results for the approximation of static force, the description of the dynamic behaviours as well as the positioning accuracy.

3.1. Approximation of Static Force

For the measurement shown here I used DMSP-20-400-RM-RM type Fluidic Muscles. In Figure 3-1 I compare the measured results with results computed with equation (2.1). The equation I worked out shows good fitting. The constant values gotten from optimization are in Table 3-1.
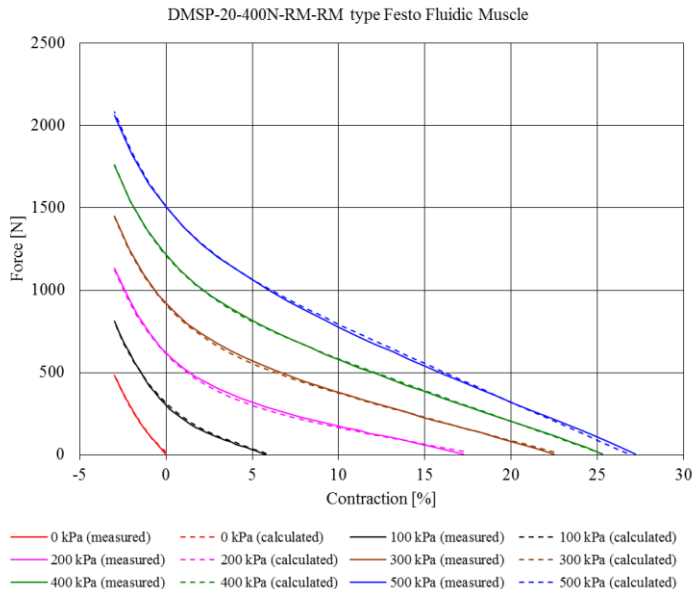

Figure 3-1: Comparison of measured and calculated results using equation (2.1)

Table 3-1: Values and confidence intervals of a_1, a_2, a_3, a_4, a_5 and a_6

Parameters	Values	Confidence intervals	
a_1	-4,35572689	-5,775448554	-2,936005225
a_2	281,2237983	278,065759	284,3818376
a_3	-0,32866293	-0,335236188	-0,322089671
a_4	-9,27034945	-9,348917301	-9,191781595
a_5	302,2010663	300,3018044	304,1003281
a_6	-263,691854	-268,3566557	-259,0270514

With equation (2.1) I got a value of R = 0,9995-0,9997 for a PAM diameter of 20 mm and R = 0,9989-0,9991 for a PAM diameter of 10 mm. We can conclude that equation (2.1) gives an accurate fitting to the measured results regardless of

diameter or length - at any given pressure (0-500 kPa). The practical implication of this presents itself at dimensioning/selecting PAMs.

3.2. Dynamic Behaviour

Using the implementation of my method built in a MATLAB Simulink model I specified - with equation (2.9) - the stiffness as a function of contraction of the 400 mm length PMI between 0-500 kPa with increments of 100 kPa (Figure 3-2). Table 3-1 shows the values for a_1, a_2, a_3, a_4. As it is shown the stiffness of the PAM is not constant and increases with pressure. The great stiffness visible at minimal contraction is decreasing with contraction and finally sets.
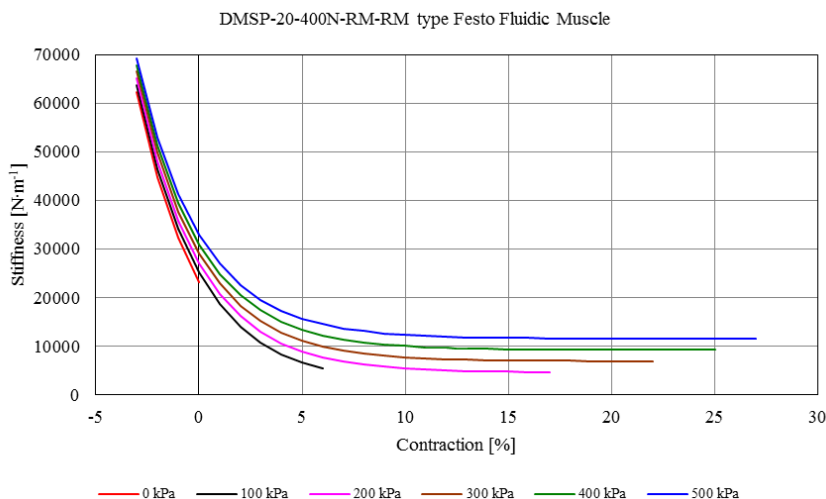

Figure 3-2: Stiffness as a function of contraction of the 400 mm length PMI between 0-500 kPa with increments of 100 kPa

The change of damping coefficient can be examined with the same MATLAB Simulink model (Figures 3-3, 3-4 and 3-5).

13

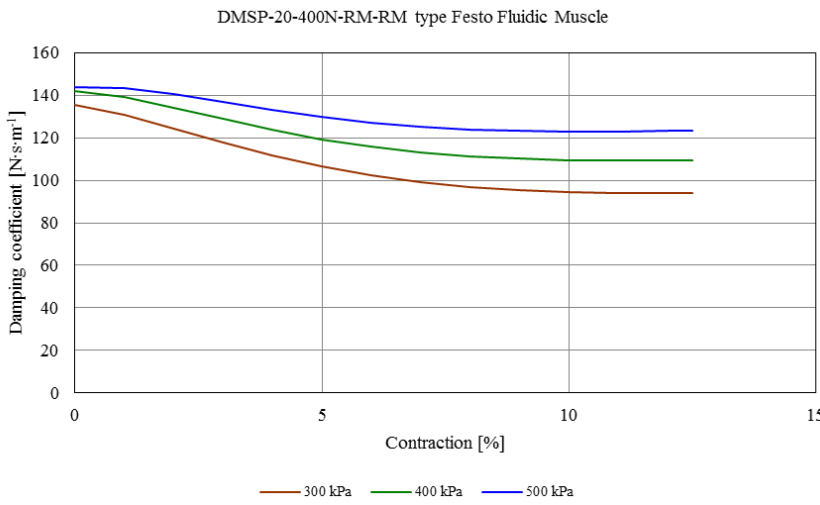DMSP-20-400N-RM-RM type Festo Fluidic Muscle

Figure 3-3: Comparison of damping coefficient with constant displacement (50 mm) but alternating loads (30 kg, 50 kg and 70 kg) and pressure (300 kPa, 400 kPa and 500 kPa)
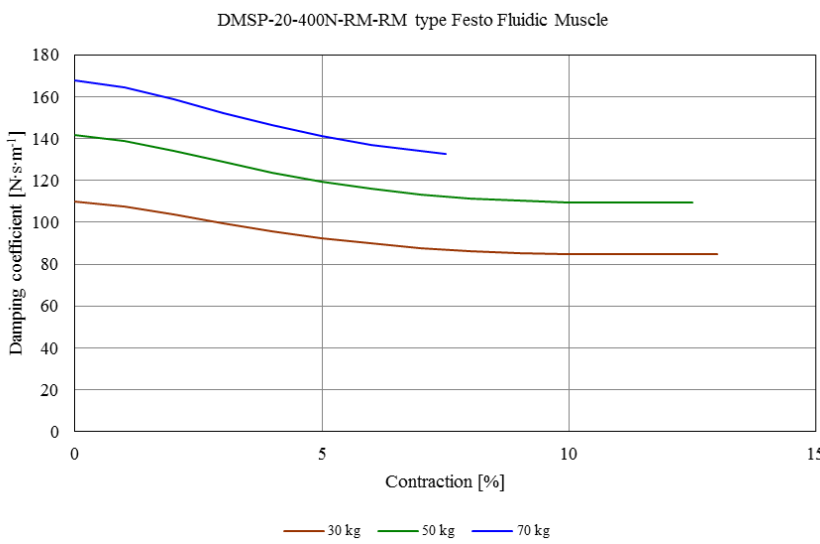
DMSP-20-400N-RM-RM type Festo Fluidic Muscle

Figure 3-4: The change of damping coefficient at constant pressure (400 kPa) as a function of contraction with loads of 30 kg, 50 kg and 70 kg.
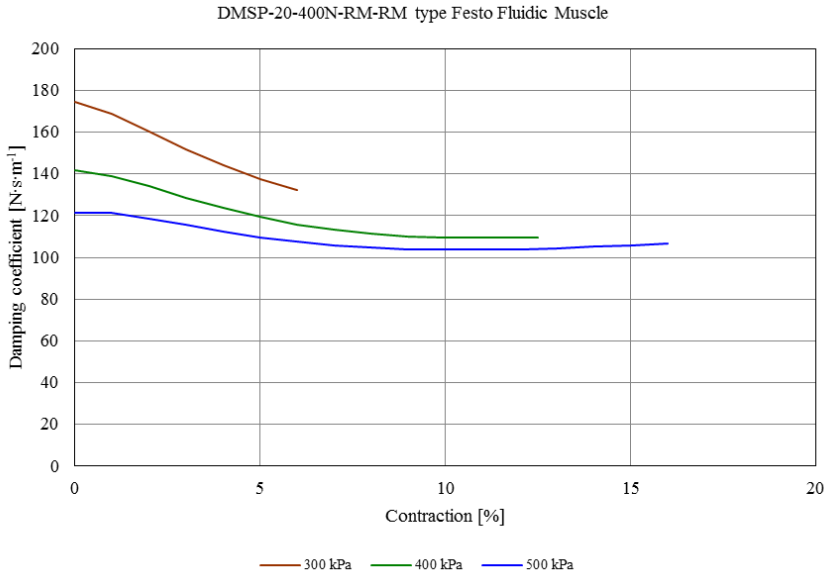
14

Figure 3-5: The change of damping coefficient as a function of contraction with a constant load (50 kg) and at values of pressure of 300 kPa, 400 kPa and 500 kPa

The MATLAB Simulink model which describes the dynamic behaviour can be used to analyse pendulous systems containing PAMs (Figure 3-6).
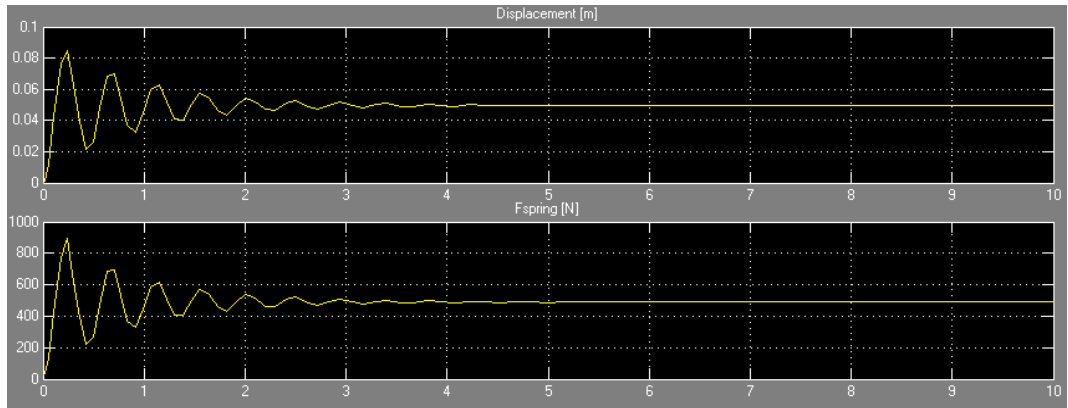
Figure 3-6: Dynamic response of pendulous system with 400 mm PAM: Displacement and F_{spring} as a function of time (400 kPa pressure, 50 mm displacement and 50 kg load)

With the simulation I ran I got 493 N F_{spring} force and 49,8 mm displacement, these results validate the method developed for the dynamic model as well as the static force model's accuracy. We can see from the presented results that the MATLAB Simulink model built according to my method is capable of describing the stiffness, damping coefficient and behaviour of the pendulous system at any working pressure (0-500 kPa) and any PAM length and diameter.

3.3. Positioning

3.3.1. Linear Positioning

During the experiments with linear displacement I installed two DMSP-20-200-RM-RM type Fluidic Muscles according to Figure 2-4. The pressure was 600 kPa the sampling time was 10 ms. The real-time acquisition of the results was done with the LabVIEW program depicted in Figure 2-5. The quality of the control (overshot, steady state error) can be influenced with the sliding surface's gradient. In my experience during the experiments the best value of the sliding surface gradient is 0,35 while the voltages of the proportional valve were: "Fast Backward" = 4 V, "Slow Backward" = 4,65 V, "In Position" = 5 V, "Slow Forward" = 5,35 V and "Fast Forward" = 6 V.
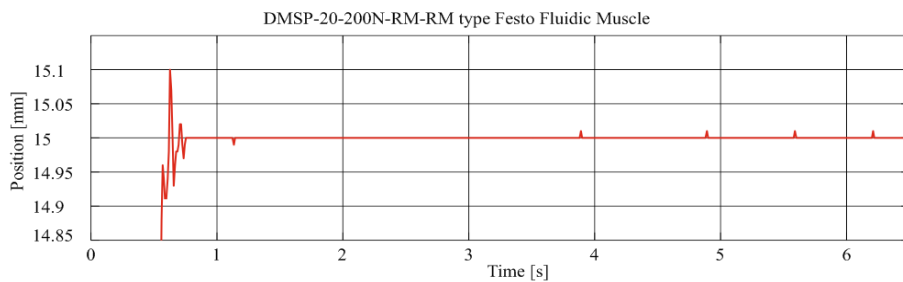

Figure 3-7: Positioning as a function of time (desired position: 15 mm)

3.3.2. Effect of Temperature and Hysteresis

I present the examination of the temperature dependence on a DMSP-20-400-RM-RM type Fluidic Muscle. Because the experimental rig can only accommodate a single 400 mm long PAM I used the configuration presented in Figure 2-6. (m = 20 kg). The air temperature entering the muscle from the compressor was 24 °C, the pressure 600 kPa, the sampling time 250 ms and the total measurement time 1200 s. On Figure 3-8 we can see the temperature change as a result of the 0,5 Hz periodic contraction. We can observe that the further I place the sensor from the pneumatic jack in other words the place where the air enters/leaves the muscle the higher temperatures I can measure we also see that while the external temperature sets around a certain points the internal temperature varies with the airflow.
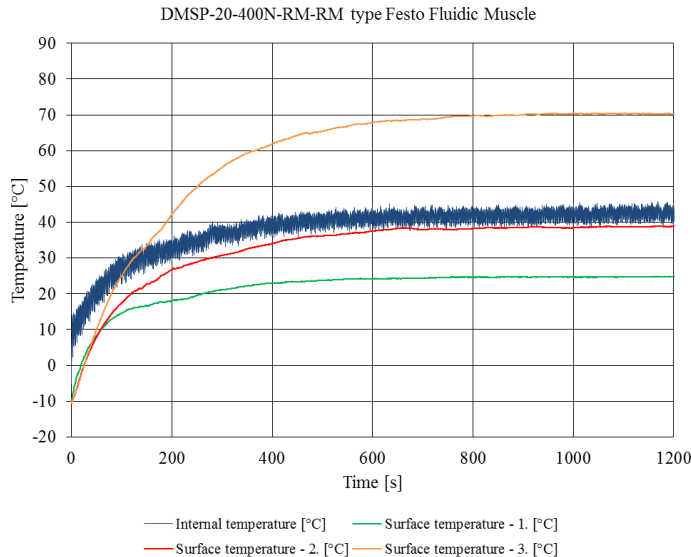
Figure 3-8: The internal and external temperature values change at a 50 Hz input signal

Table 3-2: Internal and external steady state temperature values of Fluidic Muscles driven at varying frequencies

Frequency [Hz]	Temperature [°C]			
	Internal	External - 1.	External - 2.	External - 3.
0,1	30-42	24	33	50
0,25	35-43	24	37	63
0,5	40-45	24	39	70
0,75	45-50	24	38	61
1	45-50	24	38	52

From the table we can see that by increasing the frequency the steady state internal temperature increased. The external sensor closest to the pneumatic jack measured the same temperature on all frequencies, the middle sensors readings vary a bit while the farthest measured provided the greatest values. The latter's temperature trend changed at 0,5 Hz. At 0,5 Hz we can observe a high temperature of 70 °C which can have a negative effect on the PAMs life expectancy. Regarding external temperature values the frequencies 0,1 Hz, 1 Hz and 0,25 Hz, 0,75 Hz yielded similar results.

The positioning experiments on varying temperatures used the same values for pressure, sliding surface gradient, voltages and sampling time were used as described in the previous chapter. To measure the results I took into account the middle sensors value and thus with 10 °C increments I positioned at temperatures of -10 °C, 0 °C, 10 °C, 20 °C, 30 °C and a maximum of 39 °C. Figure 3-9 shows that

at -10 °C the positioning took about 1,4 s with an overshot of 0,02 mm and a steady state error remained within 0,01 mm.
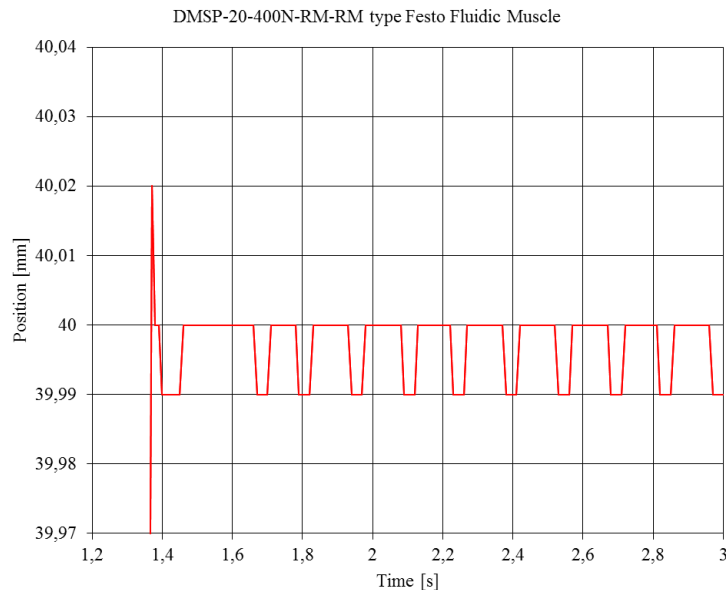

Figure 3-9: Positioning with PAM at -10 °C (desired position: 40 mm)

On Figure 3-10 we can see the result of positioning at the highest temperature achieved 39 °C. Positioning time was about 1,2 s, steady state error was within 0,01 mm.
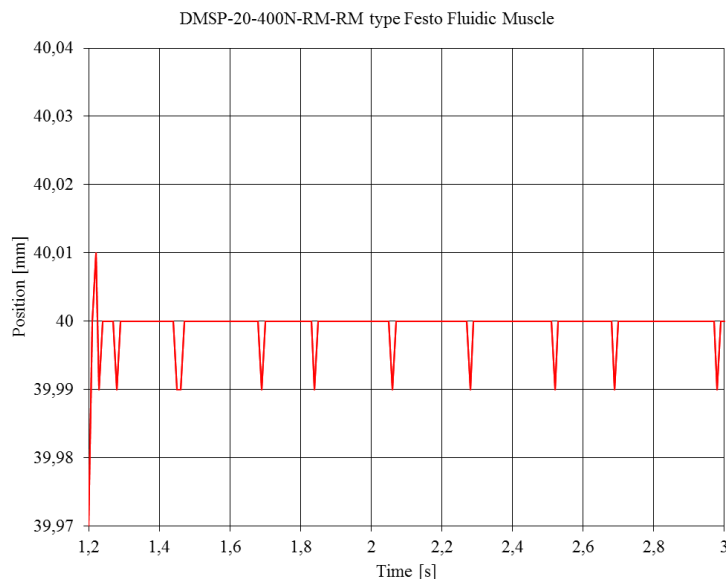

Figure 3-10: PAM positioning at 39 °C (desired position: 40 mm)

From the results we can gather that on all temperatures the positioning steady state error is within 0,01 mm. We can also see that with increased temperature the positioning time decreases. While researching the literature I have not found an author who approached or studied the subject of temperature's effect on positioning.

Along with changing temperature I examined the effect of hysteresis on the accuracy of positioning. Figure 2-6 shows the experimental setup (m = 20 kg), the gradient of the sliding surface as well as the voltages of the proportional valve match the ones used in the previous experiments. The measurement was conducted in room temperature in which I used 600 kPa of pressure and the sampling time was 10 ms. The following positions were reached in succession 0 mm (starting position) $\rightarrow$ 5 mm $\rightarrow$ 10 mm $\rightarrow$ 20 mm $\rightarrow$ 40 mm $\rightarrow$ 20 mm $\rightarrow$ 10 mm $\rightarrow$ 5 mm $\rightarrow$ 0 mm (back to starting position). As Figure 3-11 and Figure 3-12 show the control system designed by me is capable of achieving 0,01 mm steady state error regardless of direction thus we can conclude that positioning accuracy is not effected by hysteresis. From the linear positioning experiments we can also conclude that the 0,01 mm resolution incremental encoder limits the positioning accuracy.
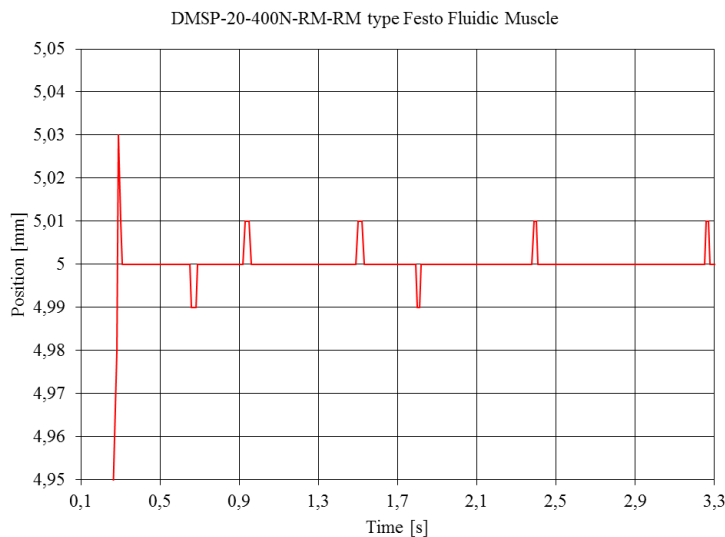
Figure 3-11: The 5 mm position's approach and hold in the increasing direction

DMSP-20-400N-RM-RM type Festo Fluidic Muscle
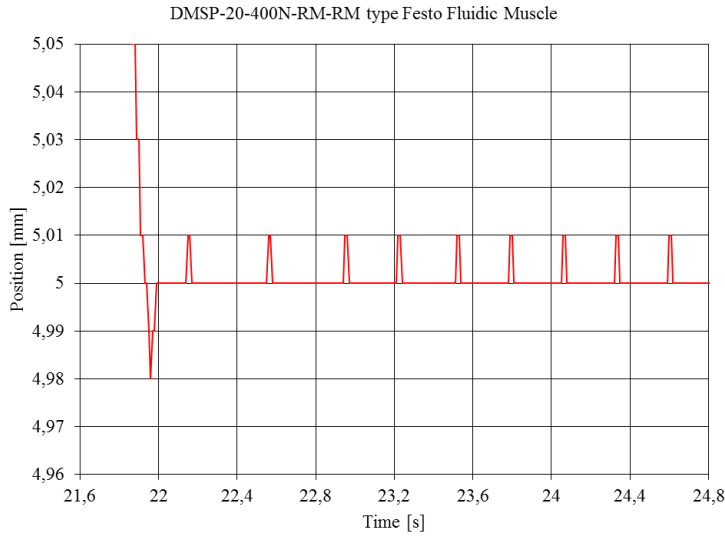
Figure 3-12: The 5 mm position's approach and hold in the decreasing direction

3.3.3. Positioning with Rotary Encoder

In the final experiments regarding positioning I examined not linear but angular displacement for which I used DMSP-10-250-RM-RM type Fluidic Muscles. The positioning was done at room temperature with 600 kPa of pressure and a sampling time of 10 ms. The gradient of the sliding surface was 0,3 while the proportional valve's voltage remained the same as before. The position of 5,004° was reached at about 0,8 s, the overshot was 0,072°, the steady state error was within 0,036° (Figure 3-13). As I concluded with linear positioning I do so here that the 0,036° resolution encoder limits the positioning accuracy.

DMSP-10-250N-RM-RM type Festo Fluidic Muscle

Figure 3-13: Positioning with rotary encoder (desired position: 5,004°)

4. NEW SCIENTIFIC RESULTS

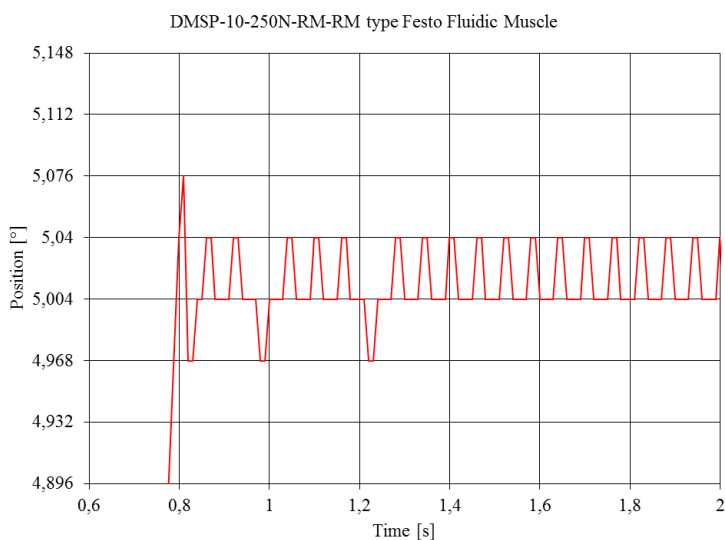1. I designed and built such an universal measurement device which is capable of measuring the most important characteristics which describe PAMs
   - force,
   - pressure,
   - position (linear and angular displacement) as well as
   - temperature.

   The generally applicable measurement and acquisition possibilities developed by me enable the rig to acquire all data for the characteristic curves of PAMs as well as conduct their high accuracy positioning. With the rig a single muscle or two muscles examination is possible. The rig is capable of producing new scientific results and it is usable in education.

2. I worked out and implemented a new model with 6 parameters for the static force which is generally applicable for any diameter and length (10 mm diameter and 250 mm length, 20 mm diameter and 200 mm length as well as 20 mm diameter and 400 mm length) muscles on any pressure (0-500 kPa):

   $$F(p,\kappa) = (a_1 \cdot p + a_2) \cdot \exp^{a_3 \cdot \kappa} + a_4 \cdot \kappa \cdot p + a_5 \cdot p + a_6,$$

   where: *a₁, a₂, a₃, a₄, a₅, a₆* unknown constants.

   I validated the accuracy of the fit (correlation coefficient: R = 0,9989-0,9997).

3. I worked out and implemented a method for the examination of the PAMs dynamic stress. The model for the solving of the second order differential equation is capable of calculating the stiffness and damping coefficient of PAMs as well as describing a total system containing PAM. At any pressure (0-500 kPa) at any PAM diameter or length (10 mm diameter/250 mm length, 20 mm diameter/200 mm length as well as 20 mm diameter/400 mm length).

4. I validated with simulations of the model describing the dynamic behaviour that a PAMs stiffness varies and it increases with pressure as a function of contraction. The stiffness observed at minimal contraction rapidly decreased with contraction finally it levelled out.

   Furthermore I proved at constant contraction, constant pressure and at constant load the damping coefficient changes:
   - at constant contraction the increasing load can only be achieved with increasing pressure which increased damping coefficient,
   - at constant pressure increasing the load increased the damping coefficient as a function of contraction,

- at constant load with increased pressure the damping coefficient decreased as a function of contraction.

5. I made a chattering free implementation of the sliding-mode control for the positioning of PAMs. With the single sliding surface designed by me I was able to achieve an accuracy of 0,01 mm linear displacement and 0,036° angular displacement. These values match the resolution of the encoders meaning a greater precision with these cannot be achieved.
One of the greatest flaws of sliding-mode control is the chattering caused by the high frequency oscillation around the sliding surface. To counter the chattering I made a barrier zone (precision zone) along the sliding surface.

6. With experimentation I proved that the designed controller is capable of eliminating the effect of varying temperature and hysteresis. I proved that the positioning time of PAMs can be shortened and also kept within the same steady state error (0,01 mm) with the increased temperature from continuous operation.

7. I proved that the working frequency of the PAMs influence the internal and external temperature of the PAM. I proved during the experiments in the 0,1-1 Hz interval that the internal temperature that sets in increases. The sensor closest to the pneumatic jack measured nearly identical values the middle one measured nearly identical and the farthest measured the highest temperatures on all frequencies. The latter's temperature trend reversed at 0,5 Hz. I observed that the contractions at 0,5 Hz caused a high temperature of 70 °C which can have a negative impact on the lifespan of the muscle. Regarding the surface temperature values for 0,1 Hz, 1 Hz and 0,25 Hz, 0,75 Hz were similar to each other.

5. CONCLUSIONS AND SUGGESTIONS

I proved with experimentation that the multifunctional test rig designed and built by me meets the set goals and expectations meaning that the most important parameters of the PAMs can be measured with the device. The programs written in LabVIEW environment provide general purpose measurement and data acquisition capabilities for measuring force, pressure, position and temperature as well as highly accurate linear and angular positioning.

With experimentation I proved an important difference between pneumatic cylinders and PAMs, while the force at cylinders is only a function of pressure and piston size meaning that at constant pressure the force does not change with position in the case of PAMs the force is influenced by displacement.

The new function for the static force of PAMs can be used to calculate without measurement the pulling force exerted by the muscle at any pressure and contraction and with the developed model describing dynamic behaviour of PAMs can be used to examine systems with PAMs.

I successfully implemented precise position control despite the nonlinearity of PAMs and their time varying properties, thus the PAMs can be used in such applications where high accuracy positioning is necessary (e.g. robot manipulators).

From the experiments we can conclude that the PAM could be used as a one directional actuator or a pneumatic spring. For bidirectional functionality can be achieved for example with a spring built in the muscle. My research in this field is currently in development.

I plan to continue my research in the field of positioning with a Balluff brand 0,001 mm resolution encoder and a National Instruments brand high performance, graphical system design compatible data acquisition and control module namely a CompactRIO. With this I will be able to measure in far greater accuracy. My examinations will extend to the 40 mm diameter Fluidic Muscles for which both the function approximation and positioning experiments will be repeated.

6. SUMMARY

In my Dissertation I dealt with different investigations of pneumatic artificial muscles (PAMs). These investigations were carried out in the laboratory of Technical Institute (beforehand Department of Technical and Process Engineering), Faculty of Engineering, University of Szeged.

My experiments were done with Festo Fluidic Muscle brand patented PAMs which come in three diameters (10, 20 and 40 mm) and up to 9000 mm in length. Their popularity is due to their favourable characteristics. Besides their force and dynamic nature they are characterized by their use in hostile environments, vibrationless operation an ease of use also their outstanding qualities include those which are analogous with human muscles such as the linear unidirectional motion and monotonic dropping force-contraction function and the antagonistic setup needed for bidirectional motion. These qualities can be found in most PAMs.

In chapter *Introduction and Objectives*, I gathered the main goals and the topics timeliness.

This is followed by chapter *Material and Method* with the next topics. An experimental setup was developed to investigate PAMs. The software components were designed in LabVIEW. New static and dynamic models were introduced here. Finally, the LabVIEW-based sliding-mode controller for accurate positioning was described.

In chapter *Results*, the results of my investigations were illustrated such as force-contraction characteristics, secondly, accurate fittings of my new models for the force were proven, next, stiffness, damping coefficient and a system using PAM were analysed with the dynamic model. Precise positioning of PAMs with 0,01 mm and 0,036° accuracies without chattering using sliding-mode control was showed. Some effects (e.g. temperature, hysteresis) on the accuracy of positioning were investigated.

In chapter *New Scientific Results*, the thesis summary of my research work was described.

Finally, chapter *Conclusions and Suggestions* is a brief abstract of my Dissertation and some conclusions and proposals on the grounds of my work were given here. Directions of this research also were designated.

7. MOST IMPORTANT PUBLICATIONS RELATED TO THE DISSERTATION

Refereed papers in foreign language:

1. Toman P., Gyeviki J., Endrődy T., Sárosi J., Véha A. (2009): Design and Fabrication of a Test-bed Aimed for Experiment with Pneumatic Artificial Muscle. International Journal of Engineering, Annals of Faculty of Engineering Hunedoara, 7 (4), pp. 91-94.
2. Sárosi J., Gyeviki J., Szabó G., Szendrő P. (2010): Laboratory Investigations of Fluid Muscles. International Journal of Engineering, Annals of Faculty of Engineering Hunedoara, 8 (1), pp. 137-142.
3. Sárosi J., Szabó G., Gyeviki J. (2010): Investigation and Application of Pneumatic Artificial Muscles. Biomechanica Hungarica, 3 (1), pp. 208-214.
4. Sárosi J., Gyeviki J. (2010): Experimental Setup for the Positioning of Humanoid Upper Arm. Analecta Technica Szegedinensia, Review of Faculty of Engineering, 2010/2-3, pp. 222-226.
5. Sárosi J. (2011): Accurate Positioning of Humanoid Upper Arm. International Journal of Engineering, Annals of Faculty of Engineering Hunedoara, 9 (Extra), pp. 33-36.
6. Sárosi J. (2011): Investigation of Positioning of Fluid Muscle Actuator Under Variable Temperature. Acta Technica Corviniensis, Bulletin of Engineering, 4 (3), pp. 105-107.
7. Sárosi J. (2012): Newest Approach to Modeling Hysteresis in the Force-Contraction Cycle of Pneumatic Artificial Muscle. Acta Technica Corviniensis, Bulletin of Engineering, 5 (4), pp. 63-66.
8. Sárosi J., Keszthelyi-Szabó G., Szendrő P. (2012): The Influence of Temperature Conditions on Position Control of Fluidic Muscle. Progress in Agricultural Engineering Sciences, 8, pp. 65-73.
9. Sárosi J. (2012): New Force Functions for the Force Generated by Different Fluidic Muscles. Transactions on Automatic Control and Computer Science, Scientific Bulletin of the „POLITEHNICA" University of Timisoara, 57 (71) (3), pp. 135-140.

Refereed papers in Hungarian:

10. Sárosi J., Gyeviki J., Szabó G., Szendrő P. (2009): Pneumatikus izmok pozícionálása csúszómód szabályozással. Gép, 60 (8), 45-48. o.
11. Sárosi J., Gyeviki J., Csikós S. (2010): Mesterséges pneumatikus izomelemek modellezése és paramétereinek szimulációja MATLAB környezetben. Jelenkori Társadalmi és Gazdasági Folyamatok, 5 (1-2), 273-277. o.
12. Sárosi J., Fabulya Z. (2013): A Fluidic Muscle által kifejtett erő közelítésének vizsgálata MS Excel környezetben. Jelenkori Társadalmi és Gazdasági Folyamatok, 8 (1-2), 70-76. o.